

# Demonstrating ARAIM on UAS using Software Defined Radio and Civilian Signal GPS L1/L2C and GLONASS G1/G2

Yu-Hsuan Chen, Adrien Perkins, Sherman Lo, *Stanford University*  
Dennis M. Akos, *University of Colorado at Boulder*  
Juan Blanch, Todd Walter, Per Enge, *Stanford University*

## ABSTRACT

As Global Navigation Satellite System continues to upgrade, the number of satellite increases and new signals in different frequencies are available. This offers users several benefits such as increased availability and improved diversity of signal. For safety-of-life users like aviation, higher availability of integrity is the key goal. A technology providing integrity with little or no ground infrastructure is receiver autonomous integrity monitoring (RAIM). As more satellites are visible to the receiver, the redundancies increase and RAIM availability for detecting faults improves. Moreover, the ionosphere delay could be eliminated through multi-frequency combination. The Advanced RAIM (ARAIM) uses multi-constellation and multi-frequency GNSS and hopes to provide vertical guidance for aircraft. For evaluating ARAIM in flight, an inexpensive flight is executed by an unmanned aircraft systems (UAS) with a developed ARAIM software receiver. The receiver supports civilian signals including GPS L1 C/A, L2C and GLONASS G1, G2. An efficient software architecture are proposed for the real-time purpose. Using the outputs from the receiver, a developed ARAIM toolbox computes the protection levels. Field test is conducted by flying the UAS on a live test campaign. The ARAIM performance during the flight shows that the vertical protection level achieves the target.

## INTRODUCTION

As ARAIM architectures are declared on ARAIM workgroup report [1], evaluating ARAIM is high-demanding. Our prior work was developing a real-time Software Defined Radio (SDR) for evaluating RAIM using single frequency and multi-constellation GNSS on the ground [2]. We tested this SDR on the roof of buildings in several locations in the world and showed the benefit of multi-constellation on geometry diversity. To extend this work to ARAIM and evaluate it in the air, we design a low-

weight GNSS SDR which can be carried on an unmanned aircraft systems (UAS). ARAIM recommends to have geometry and frequency diversity. Hence, currently full-operational constellations GPS/GLONASS and dual frequency L1/L2 are implemented in SDR. We only use civilian signals to demonstrate ARAIM performance for civilian aviation user, so GPS L2C is being used without semi-codeless technique on L1/L2. Our SDR has no protection techniques on detecting range error and ephemeris faults. The ARAIM algorithm is responsible for detecting the fault and calculating protection level.

The operational level which ARAIM hopes to achieve is LPV-200 [3]. LPV stands for localizer performance with vertical guidance. 200 means that it enables an aircraft to descend as low as 200 foot height above touchdown. Currently, the ICAO Standards And Recommended Practices (SARPs) only specifies the performance requirements for SBAS. Hence, this requirement is served as our ARAIM target. In the SARP, the vertical positioning performance criteria is 4m, 95% accuracy corresponded to Vertical Position Error (VPE). Also, 35 m, 99.99999% limit on the vertical position error corresponds to Vertical Protection Level (VPL).

The UAS is tested during an experimentation program in a military authorized area. The UAS was flew for 10 minutes. We collect the four IF signals for GPS/GLONASS L1/L2. The developed SDR does post processing from signal-processing to positioning. Its positioning results are then sent to the developed ARAIM toolbox to compute the protection level.

This paper is organized as follows. First, the testing UAS is introduced. The development of ARAIM receiver is described. Then, an overview of GNSS signal status on the testing date is given. The software architecture and integration issues are addressed. We then explain the data processing flow from receiver to ARAIM toolbox. The

testing setups and results are shown. Finally, the path forward real-time ARAIM is described.

## STANFORD JAGER UAV

The UAS executing the flight test is Stanford's JAGER UAV [4]. JAGER stands for Jammer Acquisition with GPS Exploration & Reconnaissance. It is designed to rapidly locate GPS jammers near airport area. Its airframe is a S1000 octocopter by DJI Innovations. The battery tray is designed by carbon fiber that allows to carry 16 Ah of lithium polymer batteries for a maximum power draw of 4 kW. With a 2 kg experimental payload, the craft can remain aloft for up to 20 minutes without recharging. The JAGER mounts an alternative position, navigation and timing (APNT) payload on board to navigate successfully in GPS-denied environments. For testing ARAIM, the original APNT payload is replaced by ARAIM payload which is a GPS/GLONASS dual frequency software receiver.

## ARAIM SOFTWARE RECEIVER DEVELOPMENT

The developed ARAIM receiver [5] is a PC-based software receiver [6][7][8]. The hardware architecture of receiver is depicted in figure 1 and its setup on UAS is in figure 2. The hardware of SDR are all commercial on-the-shelf components consisting of an Intel NUC NUC5i7RYH [9], two USRP B210s [10], a GPSDO, a multi-frequency GNSS antenna and a 4-way power splitter. The antenna is Maxtena's M1227HCT-A2-SMA [11], an active helix design for GPS and GLONASS L1/L2. The signal from antenna is split by 4-way power splitter and then connected to 2 USRP B210s. The USRP B210 has dual received channels sharing the common synthesizer. It can receive 30 and more MHz bandwidth which can span from GPS to GLONASS for single frequency. Two USRP B210 are programmed to receive L1 and L2 and then converted to digital intermediate frequency (IF) data, 14-bit complex or in-phase and quadrature outputs (I & Q). The RF center frequency is set to 1590 MHz for L1 and 1237 MHz for L2. The sampling rate is set to 8 Megasamples per second (MSPS). These data are transferred to NUC. The CPU equipped with Intel NUC is Core i7-5557U 5th generation Core i7 which has dual core and each core can run two threads. So, total 4 threads can be run in parallel. The PC runs the Ubuntu distribution of Linux. The USRP hardware driver (UHD) [12] is used to configure the USRP and daughter board settings such as sampling rate and RF center frequency. The digitalized IF data is then processed in real-time and stored into hard drive in the PC.

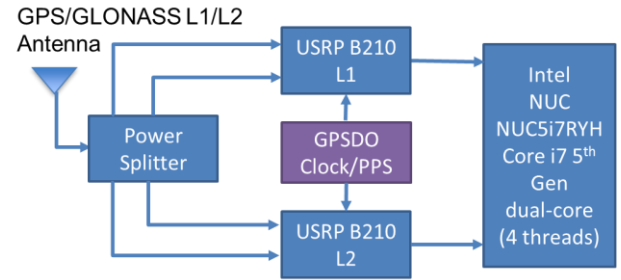


Figure 1. Block diagram of receiver



Figure 2. UAS and receiver setup

## GNSS SPECTRUM AND STATUS

With the frequency setting described in the previous section, the transmitted signal spectrum are depicted in figure 3. The spectrum contains signals from two constellations, GPS and GLONASS L1/L2. GPS L1 C/A uses Binary Phase Shift Keying (BPSK) modulation on 1575.42 MHz and 1.023 MHz chipping rate [13]. GPS L2C also uses BPSK modulation and has CM and CL code. The L2 CM code with the 50 sps symbol stream is time-multiplexed with L2 CL code at a 1023 kHz rate. Currently, we only use L2 CM code. GLONASS is using Frequency Division Multiple Access (FDMA) and there are 14 (-7 to 6) frequency channels depart by 562.5 kHz for G1 and 437.5 kHz for G2 [14]. Each channel is also modulated by a standard code (S-code) which is a Pseudo-Random Noise code with chipped rate 511 KHz. Table 1 is channel assignment in the SDR. Number 1~32 is for GPS L1 C/A PRN 1~32, 201~232 is for GPS L2C PRN 1~32, 501~514 is for GLONASS G1 -7~6 frequency channels, and 601~614 is for GLONASS G2 -7~6 frequency channels.

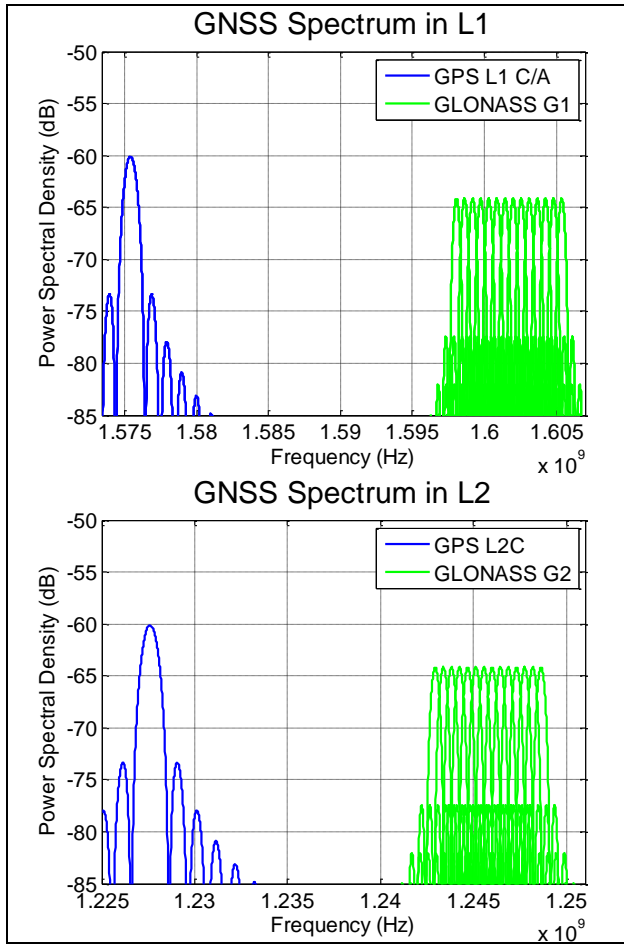


Figure 3. GNSS signal spectrum top: L1 bottom: L2

Table 1. Channel Assignment

Constellation	Satellite Number	Assigned PRN
GPS	L1 C/A 31 L2C 16	1~32 201~232
GLONASS	G1 24 G2 24	501~514 601~614

## SOFTWARE ARCHITECTURE OF RECEIVER

Because of high sampling rate 8 MSPS and four receiving channels, the software needs to be designed efficiently to achieve real-time capability [15][16][17][18][19]. The goals of software architecture are to run 4 threads in parallel and have 48 channels or 12 channels for each frequency in each constellation. The software architecture of receiver is shown in figure 4. The software starts from requesting data from the UHD driver and then store the data into a 2-second-long queue. Every 1 millisecond data is processed in 2 working threads. Each thread serves for 24 channels in which executes functions including

software correlator, signal acquisition/tracking and message decoding. These functions have the most computational complexity, so we distribute these channels to two threads for saving processing time. For every 100 millisecond, another thread makes measurement from all tracked channels and then solves the receiver position. As number of available satellite increases, the computational load of matrix multiplication inside the positioning gets higher. Hence, a dedicated thread for positioning is needed. There is an additional thread reserved for future implementation of ARAIM algorithm. By considering the complexity of ARAIM algorithm, providing 1 Hz output rate should be enough for evaluating purpose.

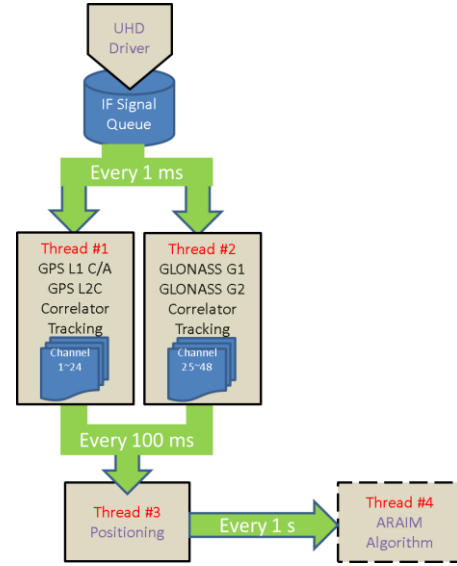


Figure 4. Software architecture

## INTEGRATION ISSUES

GLONASS's coordination system PZ-90.11 is different from the GPS WGS-84. The transformation formula between two coordination systems is

$$\begin{bmatrix} X \\ Y \\ Z \end{bmatrix}_{\text{WGS84}} = \begin{bmatrix} 1 & +0.02041 \cdot 10^{-6} & +0.01716 \cdot 10^{-6} \\ -0.02041 \cdot 10^{-6} & 1 & +0.01115 \cdot 10^{-6} \\ -0.01716 \cdot 10^{-6} & -0.01115 \cdot 10^{-6} & 1 \end{bmatrix} \begin{bmatrix} X \\ Y \\ Z \end{bmatrix}_{\text{PZ-90.11}} + \begin{bmatrix} +0.013 \\ -0.106 \\ -0.022 \end{bmatrix} \quad (i)$$

which is found in [20]. The transformation is used when integrating GLONASS satellite position to the same coordination system as GPS and then calculating position.

For adding a constellation, an extra time unknown is added to G matrix [5] because time system is different. Currently, the time offset between GPS and GLONASS is around 17 seconds corresponding to leap seconds between GPS and UTC. This offset is too large to be solved using the G matrix. Hence, our solution is to firstly eliminate the 17 seconds and then let the positioning to solve the remaining

time offset within 1 second. Two separated local times are assigned to GPS and GLONASS, respectively. These local times are corrected by the error through positioning.

When making GPS iono-free combination of dual-frequency pseudorange, the GPS ICD [13] provides the formula

$$PR = \frac{(PR_{L2C} - \gamma_{12} PR_{L1C/A}) + c(ISC_{L2C} - \gamma_{12} ISC_{L1C/A})}{1 - \gamma_{12}} - cT_{GD} \quad (2)$$

where  $PR_{L2C}$  is the pseudorange from GPS L2C,  $PR_{L1C/A}$  is the pseudorange from L1 C/A,  $ISC_{L2C}$  is the inter-signal correction between L2C and L1 P/Y,  $ISC_{L1C/A}$  is the inter-signal correction between L1 C/A and L1 P/Y,  $T_{GD}$  is the group delay correction between L1 and L2,  $\gamma_{12}$  is  $(77/60)^2$ .  $ISC_x$  is obtained by decoding CNAV message from L2C. For GLONASS,  $ISC_{G2}$ , time difference between G2 and G1 is provided by GLONASS message [14]. The GLONASS iono-free combination is

$$PR = \frac{(PR_{G2} - \beta_{12} PR_{G1}) + c(ISC_{G2})}{1 - \beta_{12}} \quad (3)$$

where  $PR_{G2}$  is the pseudorange from GLONASS G2,  $PR_{G1}$  is the pseudorange from G1,  $\beta_{12}$  is  $(1602/1246)^2$

## DATA PROCESSING FLOW

Current receiver has not implement ARAIM algorithm in real time. The ARAIM algorithm is evaluated in post-processing. The data processing flow from the receiver to ARAIM algorithm is shown in figure 5. The flow starts from running SDR and then logging required data at 10 Hz rate. The data includes residuals, G matrices, and weighting vectors from position calculation. The MATLAB ARAIM toolbox is developed based on [3] to calculate the protection level. Satellite exclusion is based on latest approach in [21]. The outputs of RAIM algorithm include Vertical Protection Level (VPL) and Horizontal Protection Level (HPL). VPL and HPL provide bounds of the Vertical Position Error (VPE) and Horizontal Position Error (HPE), respectively. As the number of satellite increases, the VPL and HPL are expected to decrease because of lower Dilution of Precision (DOP).

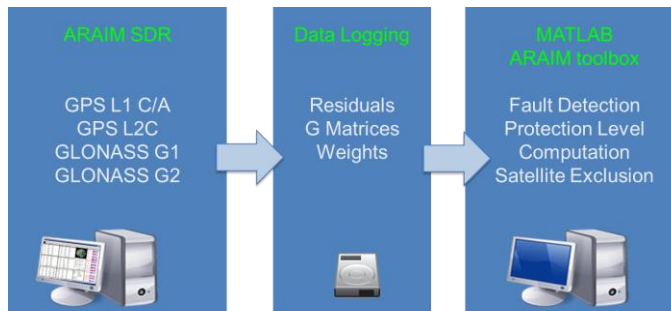


Figure 5. Data processing flow

## TESTS AND RESULTS

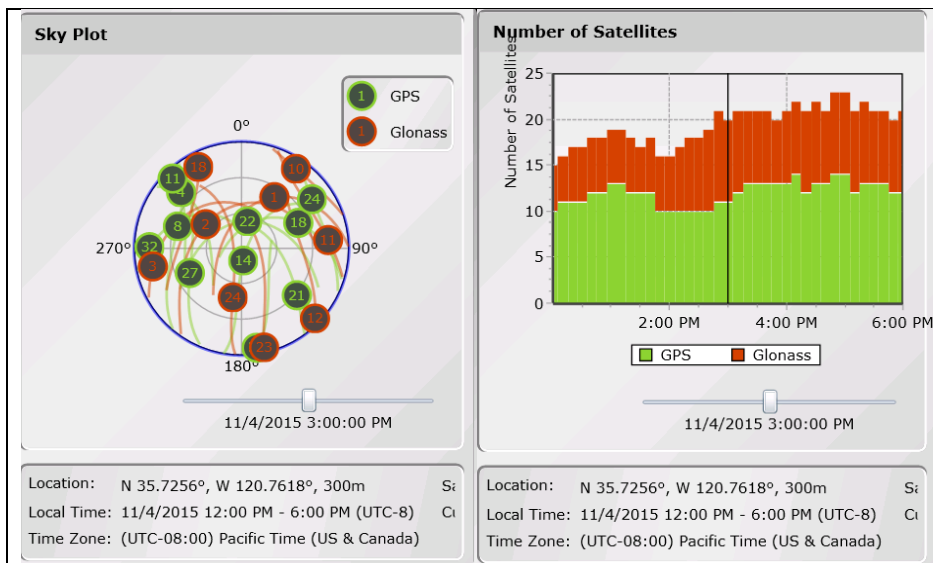
The test campaign we flew JAGER is Joint Interagency Field Experimentation Program (JIFX) taking place in Camp Roberts, California, USA on November 4, 2015 which is hosted by Naval Postgraduate School. The flight area is military authorized, so we are allowed to fly our JAGER. We launched the JAGER on a hill and total flight time is around 10 minutes. Figure 6 shows the UAS testing route and figure 7 is the testing flight picture. Figure 8 is the prediction of sky plot during test. The GPS and GLONASS dual frequency signals are successfully collected in the disk. Figure 9 is GUI of SDR in post-processing. There were 11 GPS and 9 GLONASS satellites in view. Only 4 GPS satellites broadcasted L2C signal. During flight, some strong interference sources potentially from internal hardware affect the signal quality for both frequencies. The GPS L1 C/A carrier-to-noise ratio drops around 10 dB-Hz compared to typical signal shown in figure 10 left. GLONASS G2 was interfered even worse shown in figure 10 right-bottom. Figure 10 right-top shows normal G2 spectrum for comparison. Hence, some channels of GLONASS G2 cannot be acquired.



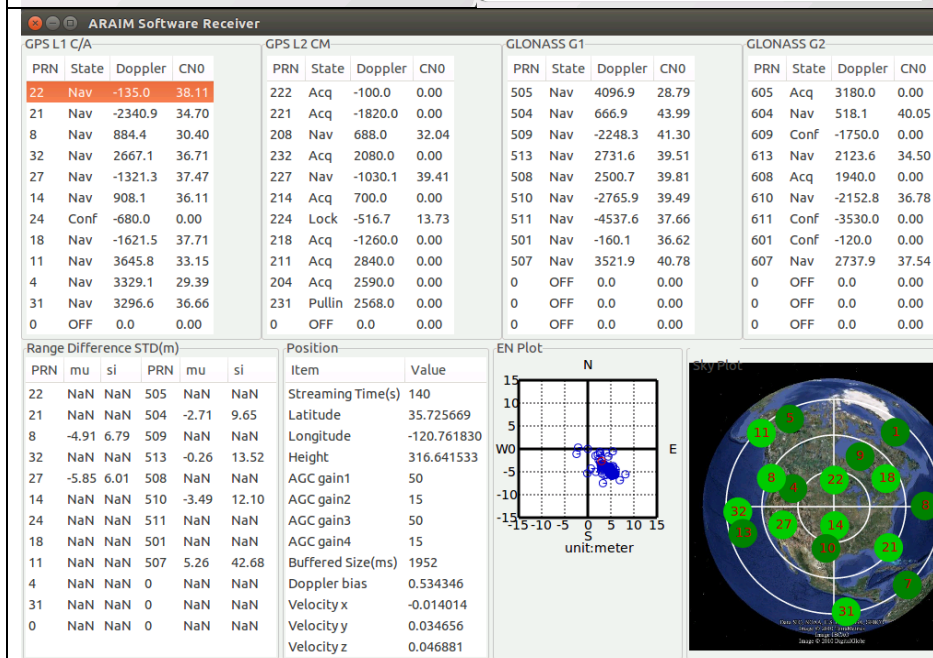
Figure 6. UAS testing route



Figure 7. UAS flight picture



**Figure 8.**  
Prediction of  
skyplot using  
Trimble GNSS  
Planning Online



**Figure 9.** GUI of  
software receiver  
in post-processing  
mode

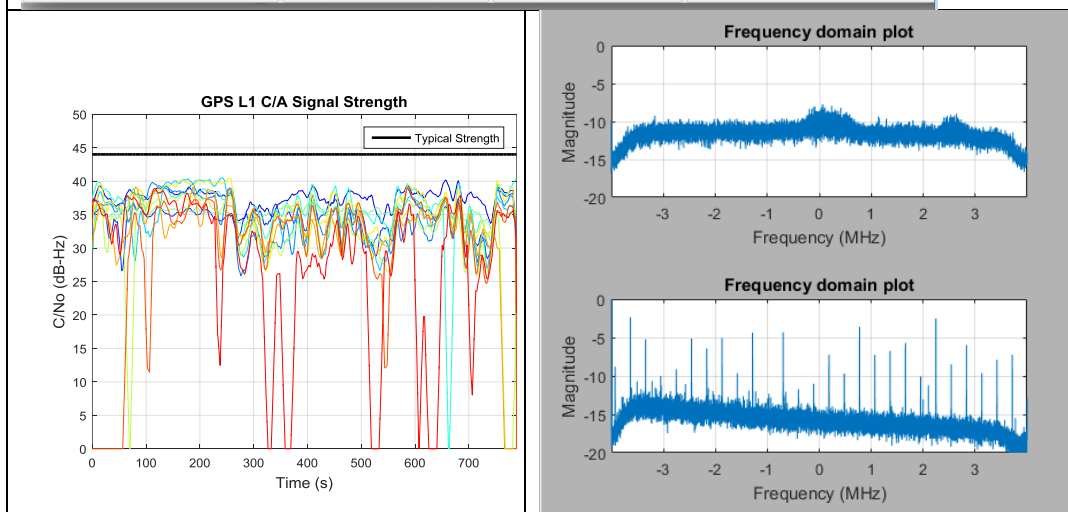


**Figure 10.**  
Left: GPS L1 C/A  
signal strength  
C/N0 during UAS  
flight  
  
Right-top: Normal  
GLONASS G2  
spectrum  
  
Right-bottom:  
Interfered  
GLONASS G2  
spectrum during  
UAS flight

Even though, our SDR still can track signal down to 25 dB-Hz by coherently integrating the whole navigation bit period and using narrow noise bandwidth in tracking loop. Figure 11 shows the satellite locked indicator during flight. For GPS L1 C/A, 11 satellites are locked almost whole flight. In the four GPS satellites broadcasted L2C, three of them are locked mostly. PRN 31 is in the low elevation angle and loses lock easily. For GLONASS G1, 9 satellites are locked. However, due to interference, 4 of 9 GLONASS G2 can be locked mostly. The strategy for pseudorange usage is if dual-frequency pseudoranges are available, iono-free combination is made. Otherwise, L1 pseudorange is used with ionospheric correction derived from Klobuchar model. The parameters of Klobuchar model are obtained from GPS L1 C/A RNAV messages. Also, the carrier smoothing/hatch filter is performed on the pseudorange with 10 seconds smoothing window.

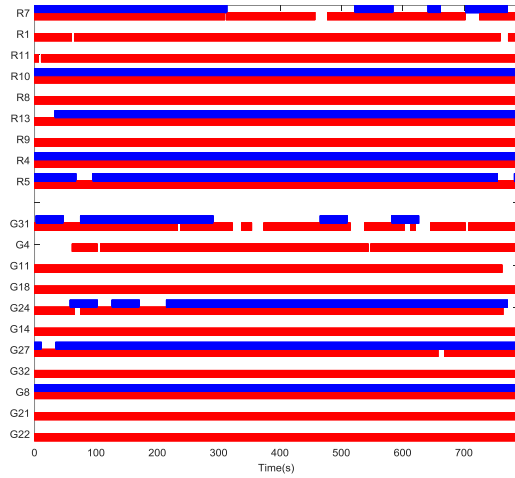


**Figure 11. Satellite locked indicator throughout UAV flight, red: L1 lock, blue: L2 lock, blank: unlock**

Figure 12 shows the vertical positioning results from three devices on UAS, ublox GPS receiver, barometer, and our SDR. The ublox GPS receiver outputs the height in mean sea level, so there is a bias to our SDR which is in ellipsoidal height. The barometer also has a 2-meter bias which is calculated from surveyed position on the ground. The vertical position errors shown later are referred to barometer height by removing the 2-meter bias. The input settings for ARAIM toolbox are listed in table 2. The VPL results of ARAIM toolbox are shown in three cases, single frequency GPS L1 C/A, single frequency GPS L1 C/A and GLONASS G1, partly dual frequency GPS L1 C/A L2C and GLONASS G1 G2. The target VPL 35m 99.99999% and VPE 4m 95% are also depicted in figures. For the single constellation and frequency shown in figure 13, both of VPL and VPE are below the target rate, especially the VPL is only 4% of time under 35m. For the single frequency and multi-constellation shown in figure 14, both of VPL and VPE achieve the target which is benefited from good geometry of satellite-receiver. For partly dual

frequency and multi-constellation shown in figure 15, VPL still achieve the target, but VPE is worse than single frequency and does not fulfill the target. This is expected in the quiet ionosphere region and quite time. Combining dual frequency pseudorange will induce more noise and multipath error than single frequency one.

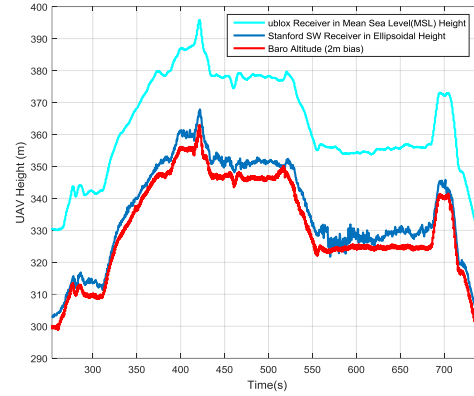


**Figure 12. Vertical positioning results from ublox GPS receiver, barometer and software receiver**

**Table 2. ARAIM input settings**

Name	Description	Value
$P_{sat}$	prior probability of fault in satellite	$10^{-5}$
$P_{con}$	prior probability of a fault affecting more than one satellite in constellation	$10^{-8}$
$\rho_{URA}$	standard deviation of the clock and ephemeris error of satellite used for integrity	2.5
$\rho_{URE}$	standard deviation of the clock and ephemeris error used for accuracy and continuity	2.5
$b_{nom}$	maximum nominal bias for satellite used for integrity	0

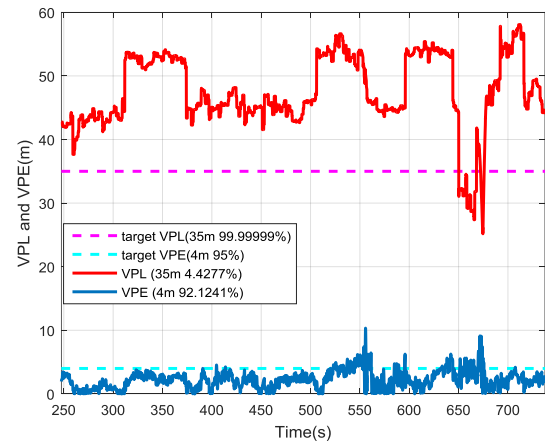


**Figure 13. VPL and VPE results for single frequency GPS L1 C/A**

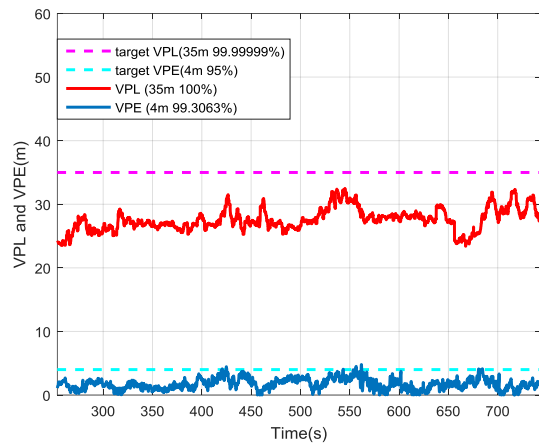


**Figure 14. VPL and VPE results for single frequency GPS L1 C/A and GLONASS G1**

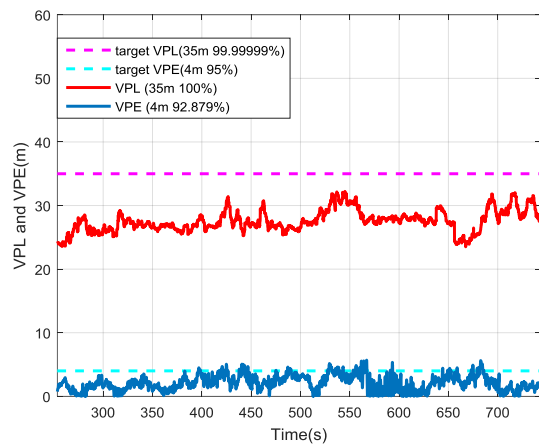


**Figure 15. VPL and VPE results for partly dual frequency GPS L1 C/A L2C and GLONASS G1 G2**

## CONCLUSIONS AND PATH FORWARD

We demonstrate an ARAIM testing on UAS in a live test campaign. The implementation of software radio for multi-constellation and dual-frequency GNSS uses the commercial off-the-shelf components. This software receiver has the repeatable advantage, so everyone with the USRP and NUC can easily repeat the same setup and conduct the same test. For ARAIM performance in the UAS flight test, the vertical position level achieves ICAO SARPs 35m (99.99999%) requirement and vertical position error achieves 4m (95%) requirement for single frequency. The results show that multi-constellation GNSS has improvement on position accuracy and protection level compared to single constellation.

For path forward real-time ARAIM, the software need to be refined using Intel's CPU new instruction set. Intel CPU Core i7-5557U supports the new SIMD instruction set AVX/AVX2 extends original register 128 bits to 256. This would accelerate computation by factor of 2. Also, AVX2

has instructions loading data by indices in parallel. Only one index table is needed to make and can be applied to any PRN code. This would reduce the memory size of code table by a factor of 32. The saving computational power will be used to implement the ARAIM algorithm.

For preventing interference, we will find the internal interference sources and add more shielding material on the enclosure. The future testing campaigns are another JIFX in May, 2016 and NavFest in White Sand, New Mexico, US in July, 2016. We will collect more data sets and test ARAIM in real-time.

## ACKNOWLEDGMENTS

The authors gratefully acknowledge the FAA for supporting this research. They acknowledge Tyler Reid from Stanford University for assistance of mounting payload. They acknowledge the Naval Postgraduate School for hosting the Joint Interagency Field Experimentation Program (JIFX).

## REFERENCES

- [1] EU-U.S. Cooperation on Satellite Navigation Working Group C-ARAIM Technical Subgroup Milestone 2 Report, available on [http://ec.europa.eu/growth/tools-databases/newsroom/cf/itemdetail.cfm?item\\_id=8191](http://ec.europa.eu/growth/tools-databases/newsroom/cf/itemdetail.cfm?item_id=8191)
- [2] Y-H. Chen, S. Lo, D.M. Akos, M. Choi, J. Blanch, T. Walter, P. Enge, "Development of a Real-time GNSS Software Receiver for Evaluating RAIM in Multi-constellation," Proceedings of the 2014 International Technical Meeting of The Institute of Navigation, San Diego, California, January 2014, pp. 525-533
- [3] J. Blanch, T. Walter, P. Enge, Y. Lee, B. Pervan, M. Rippl, A. Spletter, "Advanced RAIM user Algorithm Description: Integrity Support Message Processing, Fault Detection, Exclusion, and Protection Level Calculation," Proceedings of ION GNSS 2012, Nashville, TN, September 2012, pp. 2828-2849.
- [4] J. Spicer, A. Perkins, L. Dressel, M. James, Y.-H. Chen, D. S. De Lorenzo, P. Enge, "The JAGER Project: GPS Jammer Hunting with a Multi-Purpose UAV Test Platform," Proceedings of ION ITM 2015, Dana Point, California, January 2015, pp. 62-70.
- [5] P. Misra and P. Enge, Global Positioning System: Signals, Measurement, and Performance, 2nd Edition, Ganga-Jamuna Press, Lincoln, MA. , 2006

- [6] D.M. Akos, "A Software Radio Approach to Global Navigation Satellite System Receiver Design," PhD thesis, Ohio University, 1997
- [7] U.S. Patent No. 7,305,021, "Real-Time Software Receiver," Awarded Dec. 4, 2007, by B.M. Ledvina, M.L. Psiaki, S.P. Powell, and P.M. Kintner, Jr.
- [8] Y.-H. Chen and J.-C. Juang, "A GNSS Software Receiver Approach for the Processing of Intermittent Data," Proceedings of ION GNSS 2007, Fort Worth, TX, September 2007, pp. 2772-2777.
- [9] Intel® NUC Kit NUC5i7RYH Mini PC, Intel, reachable on the web at <http://www.intel.com/content/www/us/en/nuc/nuc-kit-nuc5i7ryh.html>
- [10] USRP B210, Ettus Research LLC, reachable on the web at <http://www.ettus.com>.
- [11] M1227HCT-A2-SMA, Maxtena Inc., reachable on the web at <http://www.maxtena.com/uploads/6/6/6/5/6665461/m1227hct-a2-sma.pdf>
- [12] UHD - USRP Hardware Driver, Ettus Research LLC, reachable on the web at [http://files.ettus.com/uhd\\_docs/manual/html/](http://files.ettus.com/uhd_docs/manual/html/).
- [13] "IS-GPS-200G", Navstar GPS Space Segment/Navigation User Interfaces, September 2012, reachable on the web at <http://www.gps.gov/technical/icwg/IS-GPS-200G.pdf>
- [14] GLONASS Interface Control Document, Russian Federation Institute of Space Device, 2008.
- [15] Y.-H. Chen, J.-C. Juang, J. Seo, S. Lo, D. M. Akos, D. S. De Lorenzo, P. Enge, "Design and Implementation of Real-Time Software Radio for Anti-Interference GPS/WAAS Sensors," Sensors 2012, 12, pp. 13417-13440.
- [16] Y.-H. Chen, D. S. De Lorenzo, J. Seo, S. Lo, J.-C. Juang, P. Enge, and D. M. Akos, "Real-Time Software Receiver for GPS Controlled Reception Pattern Array Processing," Proceedings of ION GNSS 2010, Portland, OR, September 2010, pp. 1932-1941.
- [17] Y.-H. Chen, "A Study of Geometry and Commercial Off-The-Shelf (COTS) Antennas for Controlled Reception Pattern Antenna (CRPA) Arrays," Proceedings of ION GNSS 2012, Nashville, TN, September 2012, pp. 907-914.
- [18] Y.-H. Chen, S. Lo, D. M. Akos, D. S. De Lorenzo, P. Enge, "Validation of a Controlled Reception Pattern Antenna (CRPA) Receiver Built From Inexpensive General-purpose Elements During Several Live-jamming Test Campaigns," Proceedings of ION ITM 2013, San Diego, California, January 2013, pp. 154-163.
- [19] Y.-H. Chen, J.-C. Juang, D. S. De Lorenzo, J. Seo, S. Lo, P. Enge, D.M. Akos, "Real-Time Dual-Frequency (L1/L5) GPS/WAAS Software Receiver," Proceedings of ION GNSS 2011, Portland, OR, September 2011, pp. 767-774.
- [20] Military Topographic Department of the General Staff of Armed Forces of the Russian Federation, "PZ-90.11," Moscow, 2014
- [21] J. Blanch, T. Walter and P. Enge, "A Simple Satellite Exclusion Algorithm for Advanced RAIM", to be present in Proceedings of ION ITM/PTTI 2016